



## Electricity Generation from Bamboo Nanoparticles Processed by High Energy Milling without Thermal Treatment Mixed with NaOH

Megara Munandar<sup>1,2\*</sup>, Eko Siswanto<sup>1</sup>, Winarto<sup>1</sup>, I. N. G. Wardana<sup>1</sup>

<sup>1</sup> Department of Mechanical Engineering, University Brawijaya, Malang 65145, Indonesia

<sup>2</sup> Mechanical Engineering Department, Faculty of Engineering, University Pancasila, DKI Jakarta 12640, Indonesia

Corresponding Author Email: [megara@univpancasila.ac.id](mailto:megara@univpancasila.ac.id)

Copyright: ©2024 The authors. This article is published by IIETA and is licensed under the CC BY 4.0 license (<http://creativecommons.org/licenses/by/4.0/>).

<https://doi.org/10.18280/rcma.340603>

### ABSTRACT

**Received:** 21 October 2024

**Revised:** 21 November 2024

**Accepted:** 11 December 2024

**Available online:** 28 December 2024

#### Keywords:

energy, electrolyte, heat treatment, nanomaterial, bamboo, NaOH, voltage

The purpose of this research is to utilize bamboo as an energy-harvesting material. Energy harvesters are produced from nanomaterial-sized bamboo. This research aims to make bamboo nanomaterials with a high-energy milling process without heat treatment as a producer of electrical energy. Bamboo nanomaterials contain a chemical composition of C, O, Si, and K with a more positive electrical charge. The addition of NaOH negatively charges the electrolyte solution due to the presence of OH<sup>-</sup>. The concentration of NaOH specifies the production of electricity because the energy gap decreases from 0.48 eV to 0.39 eV. During the electricity generation process, some of the Al electrodes dissolve into the electrolyte and form a more regular crystal structure so that the energy gap decreases further to 0.28 eV, which has a stronger electricity generation capacity. The electrical voltage produced in the battery cell is around 768 mV.

## 1. INTRODUCTION

Increasing economic and technological growth demands a higher energy supply. This matter results in excessive consumption of fossil fuels, resulting in increased CO<sub>2</sub> emissions that trigger global warming. This matter highly requires carbon neutrality [1, 2]. Fossil fuels remain significant in meeting current energy needs. Therefore, developing an effective and renewable energy system is a challenge. Energy is a necessity in every healthy economy [1]. Energy storage is a technology that generates renewable energy and converts it into an efficient electricity grid. The electrostatic force in electrolyte solutions can convert chemical energy into heat energy [3]. Battery development requires innovation in solutions, electrodes, work cycles, and the development of natural materials [4]. During use, the electrolyte solution sticks to the electrode surface, causing dendrites to appear [3], which can affect the service life. The need for environmentally friendly energy generation can grow, and energy storage technology can be relied on.

Nature has the potential for energy sources, both renewable and non-renewable [5, 6]. Sodium atoms are a very abundant and easily found element at low cost and can be used as a substitute for lithium in batteries [1]. In addition, the ion has a radius of 1.02 Å, and Na<sup>1+</sup> electrons in the outer shell. Sodium undergoes oxidation to 1 and an electronegativity value of 0.93. While lithium has a radius of 0.76 Å, Li<sup>1+</sup> electrons in the outer shell undergo oxidation to +1, and an electronegativity of 0.98. In addition, electrolyte decomposition and electrode degradation can reduce battery life. Sodium is more common than lithium because it is cheaper and can save costs. Bamboo

is developing into a composite material and energy producer. Bamboo has carbon, oxygen, and hydrogen components [7,8]. Atoms bond with each other by forming a honeycomb (hexagon). In addition, this content also contains hemicellulose, lignin, and cellulose [9]. The cellulose structure is formed from Van der Waals forces during natural processes so that the cellulose becomes strong (forms crystals) [10] into bamboo. Monosaccharides are the simplest carbohydrate compounds used for energy. Carbohydrate compounds have a D-glucose structure, with carbon, oxygen, and hydrogen content. Molecular bonds in carbohydrates form 1,4-beta glycosidic [11, 12] cellulose structures connected with O as long chains [8]. Oxygen binds cellulose into long chains, micro fibrils, and crystalline and noncrystalline regions. Research developments are leading to nanomaterials and fibers. Bamboo will develop towards micro materials.

Nanomaterials are the manufacture of nanoscale materials. The manufacture of nanoscale materials is divided into two: top-down and bottom-up [13]. Top-down and Bottom-up developments have weaknesses such as limited end products (size), reprocessability, long reaction times, and require large materials. Top-down is an approach to making materials into nanotechnology [3]. Nanotechnology is developing as nanocomposites, nanocrystals, carbon nanotubes, nanobands, and semiconductors (nanocrystalline). Kinetic energy gives the ball the energy to change the shape of the material. Energy ball milling can reduce particle size, increase pore volume, and modify chemical composition.

The development of materials from micro to nanomaterials requires a process called High Energy Milling (HEM). HEM is a process of materials from micro to nanomaterials, by

changing the material from crystalline to amorphous [14, 15]. The smaller the size of the material, the easier it is for collisions to occur resulting from electrostatic forces, higher strength, interatomic forces, elasticity, and chemical stability. Nanomaterials can accelerate ion migration and may increase the reversibility of conversion reactions. High Energy Milling is an approach to producing amorphous materials [16]. HEM can cause materials to become deformed, and dislocated, and materials to be destroyed or split. Steel ball induces physical and chemical properties on the surface through kinetic energy [17].

In general, the chemical structure of bamboo will change from  $C_6H_{12}O$  to  $C_6H_{12}$  when undergoing a thermal process and become activated carbon. Activated carbon can be a good material for creating energy. Bamboo is modified into nanoparticles [18] through a high-energy milling process. Steel balls change crystalline bamboo into amorphous material using the High Energy Milling process. Sodium oxide mixed with water and bamboo produces minute dipole-dipole interactions. The positive electrode will attract negatively charged electrons. The negative electrode will attract positively charged electrons. Redox reactions occur between electrodes and electrolyte solutions through the laws of thermodynamics.

Bamboo nanoparticles without heat treatment as energy harvesting materials. Energy harvesters are produced from chemical energy to get electrical energy. The energy harvester produced from bamboo nanoparticles can provide power during the day and night. The development of bamboo nanoparticles as a green energy material must have ionic conductivity, lower cost, and safety. The manufacture of green energy materials without heat treatment is a change in the structure of cellulose/phenol into activated carbon/honeycomb/benzene [19]. Therefore, energy is needed to convert bamboo into activated carbon. Cellulose in activated carbon requires heat energy to release the oxygen contained. The heat treatment process takes time and energy. The time and energy spent result in increased production process costs. Therefore, researchers are trying to reduce production costs by offering a process without heat treatment. This study aims to produce an electrolyte solution from bamboo without heat treatment will reduce production costs and last longer.

## 2. MATERIALS AND METHODS OF RESEARCH

Bamboo nanoparticles as green material. Green material is an energy-producing material in the form of electrolyte solutions. Nanoparticles can generally dissolve in various types of solutions. Sodium oxide in solution can increase the pH and the nature of the solution to become alkali as an electrolyte solution [20, 21]. Bamboo nanoparticles join in with sodium solution [22]. In this study, bamboo nanoparticles were reacted with sodium to produce energy.

### 2.1 Preparing nano bamboo material

In the first stage, the top-down method was applied to change the bamboo from large to small. Bamboo is cut into 50 cm, then split into 4-8 pieces. The bamboo is then cleaned and dried in the sun until dry. Next, the bamboo is mashed with a planer machine. The powder from the planer machine is then blended until smooth and sieved with a 200 mesh ( $74 \mu\text{m}$ )

sieve. Bamboo that has reached a size of 200 mesh is then blended further until soft and then sieved using a 400 mesh ( $37 \mu\text{m}$ ).

Figure 1 is the bamboo-making process. Bamboo particles that have reached a size of 400 mesh and crashed using the high energy milling (HEM) method, namely the process of particle collisions with balls in a chamber [23]. Bamboo that has received HEM treatment will produce chemical reactivity [24]. The HEM process is as long as  $6 \times 24$  hours with 240 cycles per minute. Particles trapped between two colliding balls will break, experience shear, and crack [25]. Centrifugal forces within the collision chamber cause particles to impact one another [26]. Continuous collisions cause nano cracks in the bamboo, and size changes to micro/nano size and production chemical reactivity.



Figure 1. Bamboo nanomaterial manufacturing

### 2.2 Electrolyte reaction

The testing stages are to make an electrolyte solution using bamboo nanoparticles and NaOH. This study used 1.20 grams of bamboo and 1.30 grams of NaOH. The first stage is to dissolve NaOH in distilled water in a measuring cup. In the second stage, bamboo with aquadest water. The NaOH solution and bamboo solution are stirred evenly in a measuring cup. The mixed solution becomes an electrolyte solution. Electrolyte solutions produce exothermic reactions, allowing the ions in the solution to move.

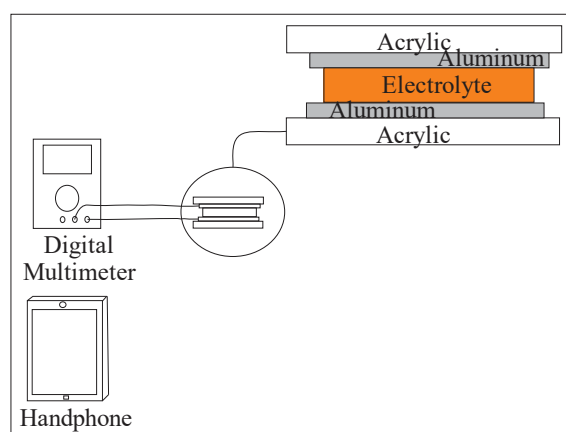


Figure 2. Electric current measurement method

Figure 2 is the process of testing electrolyte solutions in generating power. Figure 2 shows the test apparatus diagram consisting of two aluminum electrode sheets wrapped in acrylic on the top and bottom. The electrolyte solution of bamboo + NaOH solution in aquadest water is injected between the two aluminum electrodes.

The next step is the measurement of electrical voltage (V). The electrolyte solution contains cellulose, sodium, OH,  $H_2O$ ,

and H<sup>+</sup> structures. These elements play a role in producing electrical energy.

## 2.3 Chemical properties and morphology

This study aims to determine the physical, chemical, and morphological properties of the materials made by conducting tests including Scanning Electron Microscope (SEM), Energy Dispersive X-ray Spectroscopy (SEM-EDS), Fourier Transform InfraRed (FTIR), and Ultra Violet-Visible (UV-VIS) [8]. SEM testing determines the surface structure, size, and chemical composition of bamboo [8] and NaOH. Analysis using EDS (Energy Dispersive X-ray spectroscopy) and SEM-EDS testing using a Quanta FEG 650 machine equipped with an Oxford X-Act instrument as an EDS detector [8]. FTIR (Fourier Transform InfraRed Spectroscopy) testing using shimadzu IR Prestige 21 [8]. FTIR testing to measure wave absorption and functional groups contained in bamboo. Bamboo absorption length 400 - 4000 cm<sup>-1</sup>. UV-Vis testing using Specord 200 Plus, Jena Analytics. The emitted wavelength is in the range of 200 - 1100 nm. Studio material simulation looks at the size of the energy gap in the material.

## 2.4 Energy quantum

UV-Vis testing determines light absorption and wavelength. The emitted light will be absorbed by the material based on the size of the material. In addition, the absorption results also show a wavelength with a range of 200 - 800 nm. This can increase the ability of bamboo nanoparticles to interact in electrolyte solutions. Testing using bamboo samples, electrolyte solutions, and electrolytes attached to the electrode parts [8]. The results of UV-Vis testing can calculate the energy gap based on the quantum energy equation.

$$Energy = \text{Plank Contant} \times \frac{\text{Speed of light}}{\text{Wavelength}} \quad (1)$$

Eq. (1) is a formula for calculating the amount of gap energy. The amount of energy absorbed can be visible from the test results. The sample absorbs energy from the light that passes through the slit and then to the detector. UV-Vis testing measures the wavelength and measuring Homo - Lumo in kcal/mol [8, 27].

## 3. RESULTS AND DISCUSSION

### 3.1 The voltage generation from bamboo, NaOH and aluminum electrodes

Figure 3(a) shows that the bamboo + NaOH electrolyte can produce an electric voltage of around 768 mV. The voltage produced comes from the increasing temperature (thermodynamics). With increasing temperature, there is an interaction between molecules in the electrolyte solution shown in Figure 3(b). The increase in room temperature causes NaOH to vibrate and produce dipole-dipole moments. The dipole moment produces Van der Waals forces [28] and electrostatic forces are created on the ions. Na with positive/polar/oxidation ion content begins to bother with bamboo in the electrolyte solution [4]. Na as positive/polar ions, will seek negative ions and interact with attractive forces.

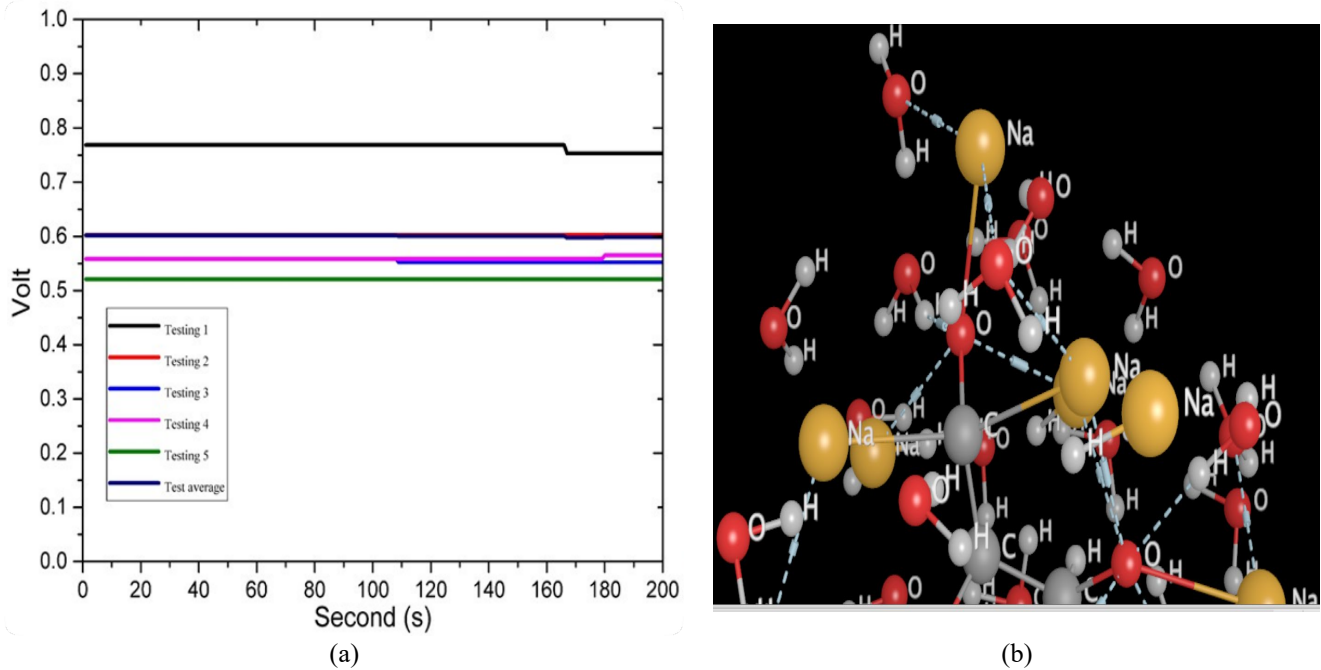
Oxidized sodium can interact with oxygen (reduction) interact with bamboo, sodium, and hydrogen. Water molecules interact with Na<sup>+</sup> cations. This interaction involves OH<sup>-</sup>, which is more often decomposed in solution [29]. Thus, Grotthuss mechanics plays a role in the occurrence of attractive forces [30]. Redox reactions occur in electrolyte solutions, causing ions to move towards the electrodes (anode and cathode).

Figure 3(a) also shows a decrease in electrical voltage with each test repetition. The largest decrease occurred between the first and second repetitions, which dropped from 768 mV to 600 mV. While from the third repetition and so on, the voltage decrease was very small and tended to be stable at around 520 mV. The increased temperature causes interaction between bamboo and NaOH. Sodium has interacted with cellulose, and there is an attractive force between [8] Na and C atoms. Thus, Na more easily releases electrons into the electrolyte solution. Bamboo has alkene, alkane, and phenol functional groups that release hydrogen [8, 31]. This will be examined in more detail with the FTIR test results in Figure 4. This mechanism was also tested using a molecular operating environment (MOE) simulation, namely a simulation to see changes in polar and nonpolar atoms. Polar atoms will experience an attractive force while nonpolar atoms will be stable as shown in Figure 3(b).

Figure 3(b) is the interaction of cellulose, sodium, and water. Bamboo has a short cellulose structure and is a natural alkane, and phenol can release hydrogen when dissolved. The released hydrogen forms a dipole-dipole moment and produces an attractive force between atoms [8], namely the Van der Waals force [28], and a new chemical bond occurs. This interaction indirectly increases the temperature. Electrolyte solutions contain [8] sodium, oxygen, potassium, and hydrogen atoms [8]. These elements can be oxidized, but some are reduced. Atoms that have polar properties can be oxidized in electrolyte solutions and move randomly or collide, increasing the temperature. Atoms that move freely in solution have hydrophilic properties, higher electronegativity, and ionization energy. Ionic interactions affect charge transfer and electrolyte mobility. The easier an atom moves, the more ionic the atom is. Sodium can improve transport and facilitate electrolyte performance [32].

Cellulose that decomposes from thermodynamic reactions circumstantially releases electrons [33]. Atomic bonds are off because their internal energy (enthalpy) is not as high as the energy in the electrolyte solution. Thus, atoms dissolved in electrolyte solutions have polar properties and are easily oxidized. Oxidized atoms try to interfere with atoms in the electrolyte solution. In addition, atoms break down into positively and negatively charged ions.

Ionic atoms C can change into cations and anions, which can attach to the electrode surface [34, 35]. Cation ions are formed on the anode surface, while anions form on the cathode surface. The ions formed can be seen from the SEM EDX test results in Figure 3. The cation ions then donate electrons to the electrode (anode), and the electrons are attracted to the electrode [8]. The electrons are then channeled by the copper conductor to the measuring instrument to read the resulting voltage. Electrons that pass through the multitester then flow to the cathode electrode and collect with anions. The anions formed have sufficient solubility in the electrolyte [36]. Oxidation causes oxygen and hydrogen to become unstable. Unstable atoms experience decreased capacity during the testing process. The advantages of aqueous electrolytes are safety factors, ion conductivity, and low cost.



**Figure 3.** Results of stress testing and calculations: (a) Resulting stress; (b) Interaction of oxygen with Na using molecular operating environment simulation

### 3.2 SEM testing

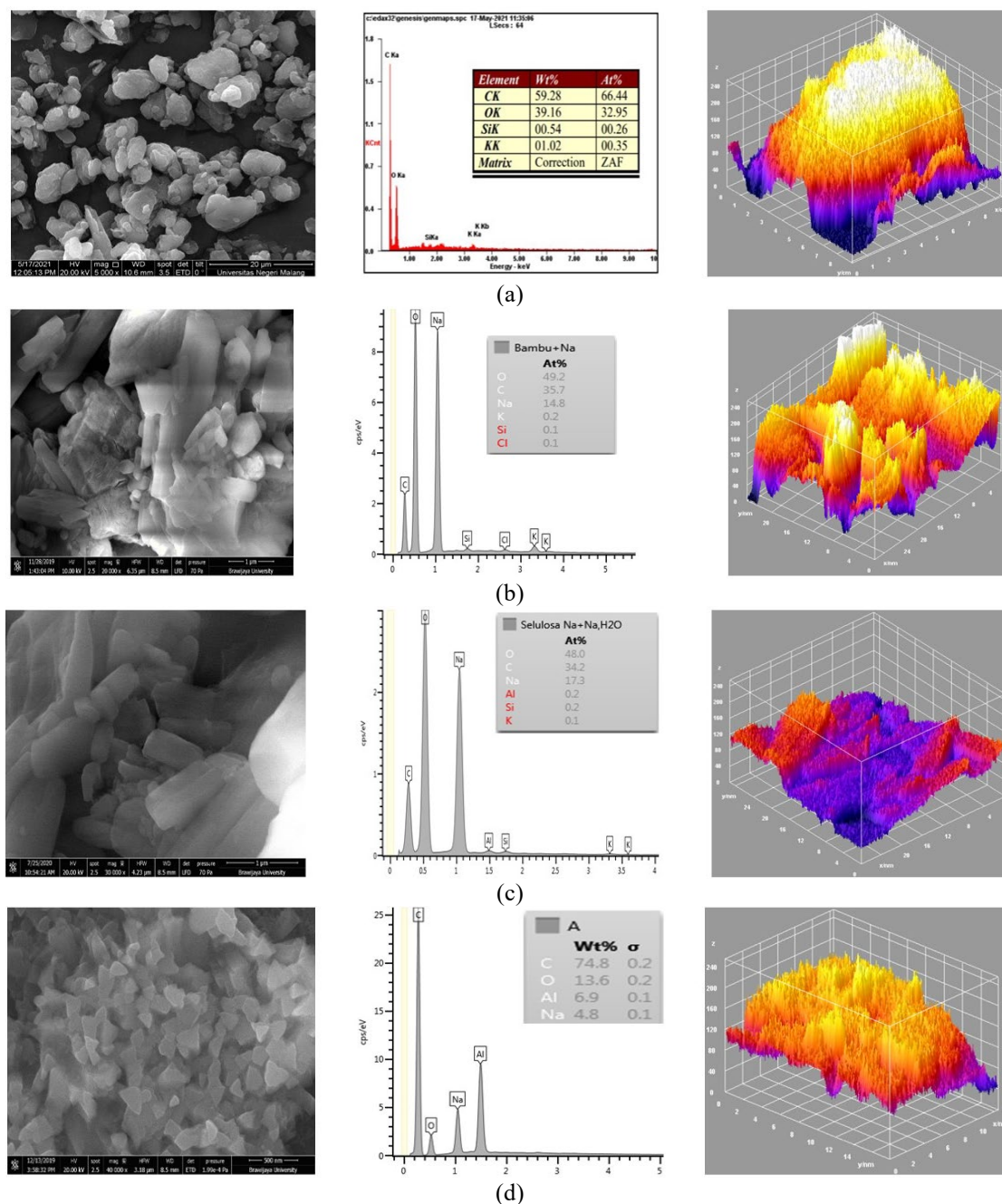
SEM-EDX testing provides an overview of the sample size of the composition contained in the material. Figure 4(a) SEM test with 20 micro magnification has various sizes. The difference in size comes from the HEM process. During the HEM process, bamboo undergoes micro cracks into nanoparticles. When the sample is tested, nanomaterials accumulate in the grains to be composed untidily. The arranged particles have amorphous properties. The results of the SEM-EDX test indicate a relatively high carbon content in bamboo. Carbon content is handy in producing energy. Figure 4(a) shows a carbon content of 59.28%, oxygen of 39.16%, silica of 0.54%, and potassium of 1.02%. Analysis with ImageJ shows a very bright surface colour of the bamboo sample. The sunny surface contour indicates the great positive ion content.

Figure 4(b) shows the results of testing cellulose mixed with NaOH. When compared to Figure 4(a) and Figure 4(b) bamboo occurs accumulation. The accumulation occurs influenced by water and NaOH. Bamboo and NaOH experience an attractive force interaction that causes bamboo and NaOH to have a long structure. Thus, bamboo and NaOH arrange themselves into long cellulose chains. The arrangement causes bamboo and NaOH to have nonpolar properties and a mixture of negative energy. The oxygen content is 49.2%, carbon 35.7%, sodium 14.8%, and potassium 0.2%. The increase in the amounts of oxygen from 39.16% to 49.2% occurs due to the addition of NaOH. The results of ImageJ analysis show a darker surface compared with pure bamboo. Indicate an increase in negative ions (electrons) in the electrolyte due to the increasing amount of OH<sup>-</sup> from NaOH.

Figure 4(c) results of testing bamboo cellulose with a higher NaOH concentration, Na increased from 14.8% to 17.3%. The results of ImageJ analysis show that the surface of the electrolyte solution becomes much darker. This shows that the

addition of NaOH can increase the number of negative ions in the electrolyte. The more negative ions the electrons are more easily excited from the valence band to the conduction band [37]. This causes the energy gap to be smaller than the molecules in the solution. The explanation will be discussed in more detail in Table 1, the following DFT simulation and UV-Vis test. The results of SEM testing showed the formation of rectangular (clusters). The formation of clusters causes the energy in bamboo to increase and negative ions to increase in the electrolyte solution. Energy and negative ions increase resulting from water and NaOH.

Figure 4(d) shows the results of electrolyte testing after the electrical energy production process between the aluminium electrodes. In Figure 4(d), the surface structure becomes small and triangular, while in Figures 4(b) and (c), the surface structures are larger and longer. After the voltage test, as shown in Figure 4(d), there is a change in the shape of the surface structure, which becomes small and triangular. The ions have flowed to the cathode and anode. So that the energy contained in the electrolyte solution is exhausted. SEM-EDS testing point that the oxygen content is 13.6%, carbon 74.8%, sodium 4.8%, and aluminium 6.9%. The SEM test results show that the size of bamboo particles is smaller than in Figure 4(c). The bamboo that has been tested releases many electrons and is caught by the electrodes during the testing process. The release of electrons causes the bamboo cellulose to decompose, and oxygen will bind to the electrode surface to become aluminium oxide. As a result, the percentage of O in the electrolyte decreases, and C increases. In part, Al electrodes are too close to the electrolyte and form alumina crystals with regular shapes as shown in the SEM photo. This regularity narrows the energy gap, which facilitates the flow of electrons to produce electrical energy. The results of the ImageJ analysis show that the color of the electrolyte surface looks brighter with a positive value compared to Figure 4(c). That indicates that the electrons in the electrolyte solution have been excited into electrical energy.



**Figure 4.** Results of Scanning Electron Microscope and ImageJ analysis: (a) Bamboo surface structure; (b) NaOH-treated bamboo surface structure; (c) Surface structure of bamboo treated with NaOH + NaOH solution; (d) Surface structure of bamboo NaOH solution + NaOH on the electrode surface

### 3.3 Functional groups

FTIR testing can determine wave absorption and functional groups. The van der Waals force formed can form cellulose. The cellulose formed will create a crystal region. The crystalline region in cellulose will form functional groups. Functional groups in cellulose include alkenes, aromatic rings, alkanes, and phenols [27]. The functional groups of alkenes C – H, aromatic rings C – H, alkanes C – H, and aromatic rings C = C [8] can release hydrogen. The hydrogen bonds released will interact with the electrolyte solution [8].

Figure 5 shows the results of FTIR testing with four (4) samples, namely bamboo (black line), bamboo + water + NaOH (red line), bamboo + water + NaOH + NaOH (blue line), and bamboo + water + NaOH + NaOH on the electrode surface

(purple line). In the first sample (black line), the alkene functional group C-H is seen at wave number 675 - 995  $\text{cm}^{-1}$ , and C-H [38] stretch at wave number 2850 - 2970  $\text{cm}^{-1}$  [39, 40], which dominates the positive ions see Figure 4(a). Figure 5 Light absorbed by nanoparticles has a short distance. This occurs in bamboo with nanoparticle size, seen from the top, and nearby bees [8].

This C-H stretch indicates that bamboo particles contain high total energy due to HEM treatment. In the second and third samples (red and blue lines), the C=C functional group appears at wave number 1610 - 1680  $\text{cm}^{-1}$  [41], and the C-H functional group at a frequency of 675–995  $\text{cm}^{-1}$ , an alkene compound. This shows that NaOH added to bamboo decomposes lignin into aromatic rings that make electrons delocalized and then excited to the surface producing the

surface of the electrolyte particles more negatively charged, and the alkene [42] functional group dominates the positive ion shown in Figures 4(b), (c). In the fourth sample (purple line), the C-H stretch functional group appears again at a frequency of 2850–2970  $\text{cm}^{-1}$ . This shows that the electrolyte (bamboo + NaOH + NaOH + water) that has been used has undergone further deformation that makes its electrons more mobile as indicated by the decrease in the energy gap, which will be discussed in Figures 6, 7, and Tables 1, 2. Figure 5 (purple line) There is a difference (red and blue lines) the difference occurs in the graph. The purple line shows the energy contained in the bamboo has been broken down into electrical energy (Figure 3). Thus, FTIR testing shows that light absorption is close. The peaks and valleys become further apart because there is energy contained in the bamboo.

### 3.4 Wavelength

Orbital DFT simulations were used to determine the band gap and Homo – Lumo for each sample. Figures 6(a) and (b) are the results of 3D simulations of the bamboo cellulose

model and the bamboo interaction model with NaOH, respectively.

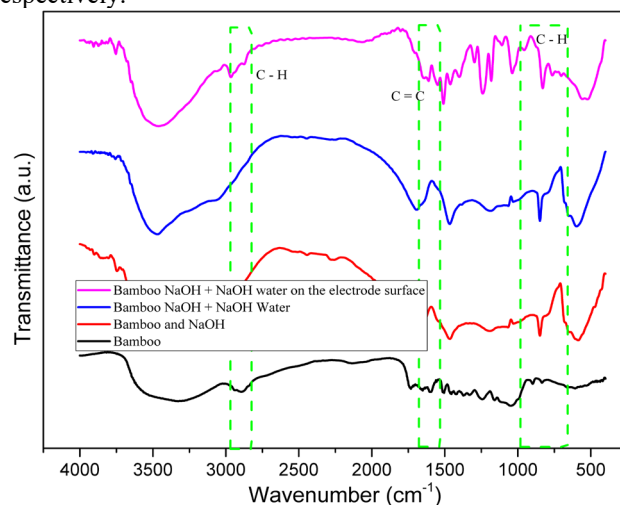


**Figure 5.** Fourier transform infrared spectroscopy test results

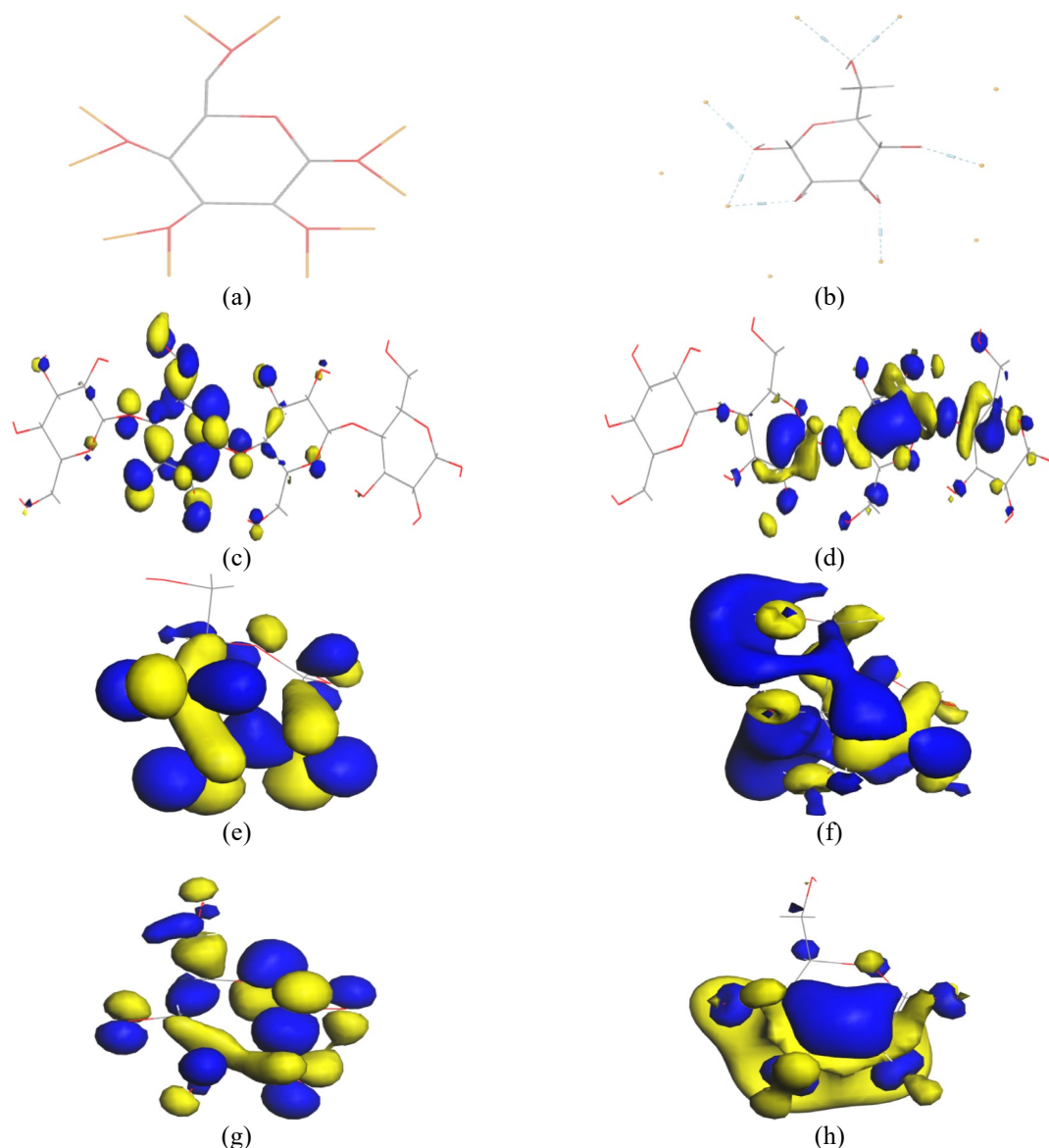


**Figure 6.** DFT orbital simulation, (a) Cellulose bamboo model, (b) Cellulose bamboo + NaOH interaction model, (c) Homo bamboo, (d) Lumo bamboo, (e) Homo bamboo + NaOH (f) Lumo bamboo + NaOH, (g) Homo bamboo + NaOH + NaOH, (h) Lumo bamboo + NaOH + NaOH

Figures 6(c)-(d) are results of DFT simulation to determine Homo – Lumo in bamboo cellulose. Table 1 bamboo shows the energy at Homo -0.2727 eV in Figure 6(c) and Lumo 0.02266 eV in Figure 6(d). Thus, the cellulose bamboo electrolyte solution has an energy gap of -0.2953 eV, the energy needed by electrons to pass through the band gap in bamboo. The energy comes from the electrostatic force in the electrolyte solution.

Figures 6(e)-(f) simulation results of bamboo+NaOH electrolyte solution. The transfer occurs in the carbon-oxygen group by binding Na atoms through the redox reaction process. The transfer of liquid Na ions is adsorption on the oxygen atoms of the O-H group [43]. Table 1 presents Homo = -0.2667

eV in Figure 6(e) and Lumo = 0.0437 eV in Figure 6(f) of bamboo+NaOH with an energy gap of -0.3104 eV.

Figures 6(g)-(h) results from the Homo-Lumo simulation of bamboo+NaOH with more NaOH added. The result of DFT simulation Table 1 bamboo+NaOH+NaOH shows Homo energy -0.2630 eV in Figure 6(g) and Lumo 0.0180 eV in Figure 6(h) with energy gap -0.2810 eV. This indicates that adding more NaOH lowers the energy gap so that electrons are more easily excited. The addition of NaOH to bamboo lowers the total energy from -2663.463858 kcal/mol to -726.149556 kcal/mol, which means the distance between atoms is getting stretched so that it is easier for electrons to be excited [8].

**Table 1.** Homo-Lumo DFT simulation

Name	HOMO	LUMO	Bandgap	Total Energy
Bamboo	-0.2727 eV	0.0226 eV	-0.2953 eV	-2663.463858 kcal/mol
Bamboo+NaOH	-0.2667 eV	0.0437 eV	-0.3104 eV	-726.098021 kcal/mol
Bamboo+NaOH+NaOH	-0.2630 eV	0.0180 eV	-0.2810 eV	-726.149556 kcal/mol

**Table 2.** Homo-Lumo energy absorption

No.	Sample	Peak Absorption (nm)	$E=hc/\lambda$ (eV)	E (eV)	Homo-Lumo (kcal/mol)
1	Bamboo	202	6.13	0.48	139
		219	5.65		
2	Bamboo + NaOH	212	5.84	0.39	132
		227	5.45		
3	Bamboo+NaOH + on the electrode surface	216	5.73	0.28	130
		227	5.45		

UV-Vis testing determines the sample's energy gap from the wavelength of light absorbed. From Figure 7, it seems that bamboo (black line) absorbs light with a wavelength of 202 nm and 219 nm. The emitted light is captured by the bamboo and then absorbed. The absorption results indicate the size of the bamboo. The smaller the size of the bamboo, the shorter the wave absorption, so it affects the energy gap. Table 1 Bamboo has an energy gap of 0.48 eV, while bamboo mixed with NaOH and aluminum has a small energy gap. The energy gap of bamboo is great and is an insulator. With the addition of NaOH, the energy gap becomes small at 0.39 eV. So bamboo has green energy properties as a result of electrical energy.

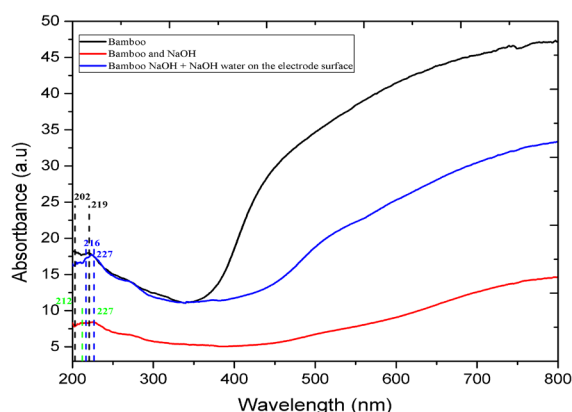


**Figure 7.** UV-Vis testing, and quantum size

Bamboo + NaOH (red line) have absorption of 212 nm and 227 nm. The results of the UV-Vis test indicate that bamboo + NaOH nanoparticles can work as semiconductor materials.

The bamboo + NaOH electrolyte sample that has been used on the electrode (blue line) shows wave absorption of 216 nm and 227 nm. From the peaks of this wavelength absorption, the energy gap for bamboo, bamboo + NaOH, and bamboo + NaOH that have been tested on the electrode as shown in Table 2. From Table 2 shows that the results of the UV-Vis test also show a tendency for the same results as the DFT simulation, namely the addition of NaOH to bamboo reduces the electrolyte energy gap. The use of bamboo + NaOH electrolyte on the electrode reduces the energy gap due to crystallization as explained by the results of the SEM test in Figure 4(d).

From here it can be revealed that the treatment of HEM cellulose bamboo into nanoparticles without thermal treatment can be an effective and environmentally friendly source of electricity generation if mixed with NaOH.

#### 4. CONCLUSIONS

1. Bamboo nanoparticles produced from the top-down process with high-energy milling without thermal treatment can produce a voltage of 768 mV when mixed with NaOH. Voltage is an improvement from increased temperature and OH- atoms with excess electron change in the electrolyte solution.

2. Increasing the amount of NaOH added to bamboo in the electrolyte further reduces the energy gap so that electrons can more easily jump to the conduction band and produce more electrical energy. The energy gap of bamboo is 0.48 eV, and the addition of NaOH solution and the energy gap of the aluminum electrode becomes 0.28 eV.

3. The interaction of bamboo electrolyte plus NaOH with aluminum electrodes results in the formation of finer and more

regular crystals due to the dissolution of aluminum into the electrolyte to form Al<sub>2</sub>O<sub>3</sub> crystals. The formation of these crystals further reduces the electrolyte energy gap so that the number of electrons flowing to the electrode becomes very high.

## ACKNOWLEDGMENT

The author would like to thank Pancasila University for the work support. The author would like to thank the Central Laboratory for Biological Sciences, Brawijaya University Laboratory of Advanced Mineral Materials, the State University of Malang, the Laboratory for the Synthesis and Application of Nanomaterials, Muhammadiyah University of Surakarta, and the Department of Mechanical Engineering, Universitas Brawijaya.

## REFERENCES

- [1] Tyagaraj, H.B., Marje, S.J., Ranjith, K.S., Hwang, S.K., Al Ghaferi, A., Chodankar, N.R., Huh, Y.S., Han, Y.K. (2023). Sodium-ion batteries: Charge storage mechanisms and recent advancements in diglyme-based electrolytes. *Journal of Energy Storage*, 74: 109411. <https://doi.org/10.1016/j.est.2023.109411>
- [2] Alvira, D., Antorán, D., Manyà, J.J. (2022). Plant-derived hard carbon as anode for sodium-ion batteries: A comprehensive review to guide interdisciplinary research. *Chemical Engineering Journal*, 447: 137468. <https://doi.org/10.1016/j.cej.2022.137468>
- [3] Montemayor Palos, C.M., Mariño-Gómez, A.E., Acosta-González, G.E., Hernández, M.B., García-Villarreal, S., Falcon Franco, L., García-Ortiz, L., Aguilar-Martínez, J. A. (2023). Large-scale production of ZnO nanoparticles by high energy ball milling. *Physica B: Condensed Matter*, 656: 3-8. <https://doi.org/10.1016/j.physb.2023.414776>
- [4] Maignan, C., Alauzun, J.G., Flahaut, E., Monconduit, L., Boury, B. (2024). Graphene oxide composites: A versatile material used as protective layer, solid-state electrolyte, and gel electrolyte in metal batteries. *Chemical Engineering Journal*, 485: 149616. <https://doi.org/10.1016/j.cej.2024.149616>
- [5] Mamoor, M., Li, Y., Wang, L., Jing, Z., Wang, B., Qu, G., Kong, L., Li, Y., Guo, Z., Xu, L. (2023). Recent progress on advanced high energy electrode materials for sodium ion batteries. *Green Energy Resources*, 1: 100033. <https://doi.org/10.1016/j.gerr.2023.100033>
- [6] Qin, Q., Zhong, F., Song, T., Yang, Z., Zhang, P., Cao, H., Niu, W., Yao, Z. (2023). Optimization of multiscale structure and electrochemical properties of bamboo-based porous activated biochar by coordinated regulation of activation and air oxidation. *Chemical Engineering Journal*, 477: 146763. <https://doi.org/10.1016/j.cej.2023.146763>
- [7] Zhang, Q., Zhang, X., He, W., Xu, G., Ren, M., Liu, J., Yang, X., Wang, F. (2019). In situ fabrication of Na<sub>3</sub>V<sub>2</sub>(PO<sub>4</sub>)<sub>3</sub> quantum dots in hard carbon nanosheets by using lignocelluloses for sodium ion batteries. *Journal of Materials Science and Technology*, 35(10): 2396-2403. <https://doi.org/10.1016/j.jmst.2019.06.002>
- [8] Munandar, M., Siswanto, E., Winarto, Wardana, I.N.G. (2024). Batteries with liquid electrolyte using bamboo, limestone and turmeric. *Annales de Chimie - Science des Matériaux*, 48(4): 571-584. <https://doi.org/10.18280/acsm.480414>
- [9] Biswas, S., Rahaman, T., Gupta, P., Mitra, R., Dutta, S., Kharlyngdoh, E., Guha, S., Ganguly, J., Pal, A., Das, M. (2022). Cellulose and lignin profiling in seven, economically important bamboo species of India by anatomical, biochemical, FTIR spectroscopy and thermogravimetric analysis. *Biomass and Bioenergy*, 158: 106362. <https://doi.org/10.1016/j.biombioe.2022.106362>
- [10] Arfin, T., Tarannum, A. (2018). Engineered nanomaterials for industrial application: An overview. *Handbook of Nanomaterials for Industrial Applications*, 2018: 127-134. <https://doi.org/10.1016/B978-0-12-813351-4.00006-7>
- [11] Xu, T., Liu, K., Sheng, N., Zhang, M., Liu, W., Liu, H., Dai, L., Zhang, X., Si, C., Du, H., Zhang, K. (2022). Biopolymer-based hydrogel electrolytes for advanced energy storage/conversion devices: Properties, applications, and perspectives. *Energy Storage Materials*, 48: 244-262. <https://doi.org/10.1016/j.ensm.2022.03.013>
- [12] Seta, F.T., An, X., Liu, L., Zhang, H., Yang, J., Zhang, W., Nie, S., Yao, S., Cao, H., Xu, Q., Bu, Y., Liu, H. (2020). Preparation and characterization of high yield cellulose nanocrystals (CNC) derived from ball mill pretreatment and maleic acid hydrolysis. *Carbohydrate Polymers*, 234: 115942. <https://doi.org/10.1016/j.carbpol.2020.115942>
- [13] Ngafwan, N., Wardana, I.N.G., Wijayanti, W., Siswanto, E. (2018). The role of NaOH and papaya latex bio-activator during production of carbon nanoparticle from rice husks. *Advances in Natural Sciences: Nanoscience and Nanotechnology*, 9(4): 045011. <https://doi.org/10.1088/2043-6254/aaf3af>
- [14] Martinez-Garcia, A., Fink, L., Bayarjargal, L., Winkler, B., Juarez-Arellano, E.A., Navarro-Mtz, A.K. (2024). Structural analysis of potato starch transformation during high-energy ball-milling: Oxygen and humidity content effects. *International Journal of Biological Macromolecules*, 260: 129579. <https://doi.org/10.1016/j.ijbiomac.2024.129579>
- [15] Zhao, J., Bian, B., Wang, X., Xie, Y., Shao, Y., Wang, C., Shao, L., Yong, Q., Ling, Z. (2024). Integrating ball milling assisted enzymatic hydrolysis of bamboo cellulose for controllable production of xylo-oligosaccharides, monosaccharides and cellulose nanofibrils. *Industrial Crops and Products*, 209: 118024. <https://doi.org/10.1016/j.indcrop.2024.118024>
- [16] Li, B., He, L., Guo, Y., Zhao, H., Shen, J., et al. (2023). High energy ball milling to synthesize transition metal vanadates with boosted lithium storage performance. *Materials Today Communications*, 37: 107496. <https://doi.org/10.1016/j.mtcomm.2023.107496>
- [17] Lopez-Tenllado, F.J., Motta, I.L., Hill, J.M. (2021). Modification of biochar with high-energy ball milling: Development of porosity and surface acid functional groups. *Bioresource Technology Reports*, 15: 100704. <https://doi.org/10.1016/j.biteb.2021.100704>
- [18] Sun, H., Li, X., Li, H., Hui, D., Gaff, M., Lorenzo, R. (2022). Nanotechnology application on bamboo materials: A review. *Nanotechnology Reviews*, 11(1): 1670-1695. <https://doi.org/10.1515/ntrev-2022-0101>
- [19] Qiu, G., Miao, Z., Guo, Y., Xu, J., Jia, W., Zhang, Y.,



- Guo, F., Wu, J. (2022). Bamboo-based hierarchical porous carbon for high-performance supercapacitors: The role of different components. *Colloids and Surfaces A: Physicochemical and Engineering Aspects*, 650: 129575. <https://doi.org/10.1016/j.colsurfa.2022.129575>
- [20] Lin, Y., Peng, Q., Chen, L., Zuo, Q., Long, Q., Lu, F., Huang, S., Chen, Y., Meng, Y. (2024). Organic liquid electrolytes in sodium-based batteries: Actualities and perspectives. *Energy Storage Materials*, 67: 103211. <https://doi.org/10.1016/j.ensm.2024.103211>
- [21] Fatima, H., Zhong, Y., Wu, H., Shao, Z. (2021). Recent advances in functional oxides for high energy density sodium-ion batteries. *Materials Reports: Energy*, 1(2): 100022. <https://doi.org/10.1016/j.matre.2021.100022>
- [22] Sahoo, R., Pal, A., Pal, T. (2016). 2D materials for renewable energy storage devices: Outlook and challenges. *Chemical Communications*, 52(93): 13528-13542. <https://doi.org/10.1039/c6cc05357b>
- [23] Youh, M., Chung, M., Tai, H., Chen, C., Li, Y. (2021). Fabrication of carbon quantum dots via ball milling and their application to bioimaging. *Mendeleev Communications*, 31(5): 647-650. <https://doi.org/10.1016/j.mencom.2021.09.018>
- [24] Choi, D., Lim, S., Han, D. (2021). Advanced metal-organic frameworks for aqueous sodium-ion rechargeable batteries. *Journal of Energy Chemistry*, 53: 396-406. <https://doi.org/10.1016/j.jechem.2020.07.024>
- [25] Jianxing, Z., Zongyu, F., Jianhui, S., He, Z., Juanyu, Y., Ning, W., Fang, C., Lei, D., Xiaowei, H. (2021). Crystal defects and phase transitions of nanocrystalline yttria-stabilised zirconia induced by high-energy ball milling. *Ceramics International*, 47(12): 16432-16440. <https://doi.org/10.1016/j.ceramint.2020.11.044>
- [26] Faraji, G., Kim, H. S., Kashi, H. T. (2018). Introduction. In *Severe Plastic Deformation*, pp. 1-17. <https://doi.org/10.1016/b978-0-12-813518-1.00020-5>
- [27] Astuti, E.S., Sonief, A.A., Sarosa, M., Ngafwan, N., Wardana, I.N.G. (2022). Synthesis, characterization and energy gap of silica quantum dots from rice husk. *Bioresource Technology Reports*, 20: 101263. <https://doi.org/10.1016/j.biteb.2022.101263>
- [28] Singh, A.K. (2016). Chapter 2-Structure, Synthesis, and Application of Nanoparticles. *Engineered Nanoparticles*, pp. 19-76. <https://doi.org/10.1016/B978-0-12-801406-6.00002-9>
- [29] Sekar, P., Ramadoss, A., Balasubramaniam, S. (2023). Tailoring potential window of aqueous electrolyte via steric molecular engineering for high voltage supercapacitors. *Applied Materials Today*, 32: 101845. <https://doi.org/10.1016/j.apmt.2023.101845>
- [30] Negara, K.M.T., Hamidi, N., Widhiyanuriyawan, D., Wardana, I.N.G. (2020). Development of energy harvesting with water droplet continuous flow over nanohollow and nanostalagmite of taro leaf surface. *Eastern-European Journal of Enterprise Technologies*, 5(5-107): 14-22. <https://doi.org/10.15587/1729-4061.2020.214263>
- [31] Wu, K., Feng, S., Hedoux, A., Shalaev, E. (2022). Water structure in glycerol: Spectroscopic and computer simulation investigation of hydrogen bonding and water clustering. *Journal of Molecular Liquids*, 355: 118916. <https://doi.org/10.1016/j.molliq.2022.118916>
- [32] Baslak, C., Demirel, S., Kocyigit, A., Erdal, M.O., Yildirim, M. (2023). Electrolyte performance of green synthesized carbon quantum dots from fermented tea for high-speed capacitors. *Diamond and Related Materials*, 139: 110275. <https://doi.org/10.1016/j.diamond.2023.110275>
- [33] Xia, W., Mahmood, A., Zou, R., Xu, Q. (2015). Metal-organic frameworks and their derived nanostructures for electrochemical energy storage and conversion. *Energy and Environmental Science*, 8(7): 1837-1866. <https://doi.org/10.1039/c5ee00762c>
- [34] Olabi, A.G., Wilberforce, T., Sayed, E.T., Abo-Khalil, A.G., Maghrabie, H.M., Elsaid, K., Abdelkareem, M.A. (2022). Battery energy storage systems and SWOT (strengths, weakness, opportunities, and threats) analysis of batteries in power transmission. *Energy*, 254: 123987. <https://doi.org/10.1016/j.energy.2022.123987>
- [35] You, Y., Manthiram, A. (2018). Progress in high-voltage cathode materials for rechargeable sodium-ion batteries. *Advanced Energy Materials*, 8(2): 1-11. <https://doi.org/10.1002/aenm.201701785>
- [36] Wu, P., Wu, S., Sun, D., Tang, Y., Wang, H. (2021). A review of Al alloy anodes for Al-air batteries in neutral and alkaline aqueous electrolytes. *Acta Metallurgica Sinica (English Letters)*, 34: 309-320. <https://doi.org/10.1007/s40195-020-01140-x>
- [37] Clarke, W.R., Simmons, M.Y., Liang, C.T. (2011). 1.08-Ballistic transport in 1D GaAs/AlGaAs heterostructures. *Comprehensive Semiconductor Science and Technology*, pp. 279-325. <https://doi.org/10.1016/B978-0-44-453153-7.00082-1>
- [38] Puja, I.G.K., Wardana, I.N.G., Irawan, Y.S., Choiron, M.A. (2018). The role of Carica papaya latex and aluminum oxide on the formation of carbon nanofibre made of coconut shell. *Advances in Natural Sciences: Nanoscience and Nanotechnology*, 9(3): 035021. <https://doi.org/10.1088/2043-6254/aad1a9>
- [39] Leng, Y., Dong, S., Chen, Z., Sun, Y., Xu, Q., Ma, L., He, X., Hai, C., Zhou, Y. (2024). Preparation of high-performance anode materials for sodium-ion batteries using bamboo waste: Achieving resource recycling. *Journal of Power Sources*, 613: 234826. <https://doi.org/10.1016/j.jpowsour.2024.234826>
- [40] Van Nguyen, D., Nguyen, H.T.N. (2023). High carboxyl content cellulose nanofibers from banana peel via one-pot nitro-oxidative fabrication. *Revue des Composites et des Matériaux Avancés*, 33(2): 127-133. <https://doi.org/10.18280/rcma.330208>
- [41] Budiyanoro, C., Yudhanto, F. (2024). Comparative analysis of cellulose, hemicellulose and lignin on the physical and thermal properties of wood sawdust for bio-composite material fillers. *Revue des Composites et des Matériaux Avancés*, 34(1): 109-116. <https://doi.org/10.18280/rcma.340114>
- [42] Ouellette, R.J., Rawn, J.D. (2018). 13-Electrophilic Aromatic Substitution. In *Organic Chemistry (Second Edition)*. Academic Press. <https://doi.org/10.1016/B978-0-12-812838-1.50013-X>
- [43] Xu, D., Sun, J., Ding, Y., Yan, A., Niu, Y., Yang, X., Zhou, Y., Gao, E., Xu, S. (2024). Highly functional molten sodium hydroxide-BaZrO<sub>3</sub> composite electrolyte with hybrid ionic conductivity for low-temperature solid oxide fuel cells. *Journal of Power Sources*, 609: 234652. <https://doi.org/10.1016/j.jpowsour.2024.234652>